Inorganic Chemistry
Article

Inorg. Chem. **2010**, *49*, 5371–5376 **5371**
DOI: 10.1021/ic100588d

Photophysical Properties, DNA Photocleavage, and Photocytotoxicity of a Series of Dppn Dirhodium(II,II) Complexes

Lauren E. Joyce,[†] J. Dafhne Aguirre,[‡] Alfredo M. Angeles-Boza,[‡] Abdellatif Chouai,[‡] Patty K.-L. Fu,[§] Kim R. Dunbar,*[,‡] and Claudia Turro*[,†]

[†]*Department of Chemistry, The Ohio State University, Columbus, Ohio 43210,* [‡]*Department of Chemistry, Texas A&M University, College Station, Texas 77843, and* [§]*Governors State University, University Park, Illinois 60484*

Received March 29, 2010

A series of dirhodium(II,II) complexes of the type *cis*-$[Rh_2(\mu\text{-}O_2CCH_3)_2(dppn)(L)]^{2+}$, where dppn = benzo[*i*]dipyrido-[3,2-*a*:2′,3′-*h*]quinoxaline and L = 2,2′-bipyridine (bpy, **1**), 1,10-phenanthroline (phen, **2**), dipyrido[3,2-*f*:2′3′-*h*]-quinoxaline (dpq, **3**), dipyrido[3,2-*a*:2′,3′-*c*]phenazine (dppz, **4**), and dppn (**5**), were synthesized and their photophysical properties investigated to probe their potential usefulness as photodynamic therapy agents. The ability of the complexes to bind and photocleave DNA was also probed, along with their toxicity toward human skin cells in the dark and when irradiated with visible light. Nanosecond time-resolved absorption measurements established that the lowest energy excited state in **1**−**5** is dppn-localized $^3\pi\pi^*$ with lifetimes of 2.4−4.1 μs in DMSO, with spectral features similar to those of the free dppn ligand (τ = 13.0 μs in $CHCl_3$). Complexes **1**−**4** photocleave DNA efficiently via a mechanism that is mostly mediated by reactive oxygen species, including $^1O_2$ and O_2^-. The DNA photocleavage by **5** is significantly lower than those measured for **1**−**4** in air, and the absence of O_2 in solution or the addition of azide, SOD (superoxide dismutase), or D_2O does not affect the efficiency of the photocleavage reaction. The toxicity of **1**−**5** toward Hs-27 human skin fibroblasts is significantly greater upon irradiation with visible light than in the dark. In contrast to the DNA photocleavage results, **5** exhibits the largest increase in toxicity upon irradiation within the series. These results are explained in terms of the known ability of the complexes to transverse cellular membranes, the toxicity of the complexes in the dark, and their photophysical properties.

Introduction

Photodynamic therapy (PDT) has received significant attention owing to the ability of the technique to target tumor tissue selectively through irradiation of the affected area.[1−7] In general, photoactivation of PDT drugs in the presence of oxygen results in reactive species, largely believed to be $^1O_2$ (singlet oxygen), although superoxide and hydroxyl radicals may also be involved in the photochemistry.[1−7] When oxygen is available, $^1O_2$ generated by the photoactivated drugs can cause oxidative damage to biomolecules including proteins, nucleic acids, and membrane lipids.[1−7] One particular drawback of these systems is that in the absence of oxygen the excited states themselves are not reactive. Therefore, when oxygen in the vicinity of the photosensitizer is consumed, the drug becomes inactive until a replenished supply of O_2 can diffuse into the cells or region of the tumor.[1−7] In addition, the most aggressive and drug-resistant tumors are hypoxic, thereby rendering these PDT drugs less effective toward them.[8] Therefore, the discovery of new PDT agents whose action does not depend on the availability of oxygen is a highly desirable goal.

Cationic dirhodium(II,II) complexes have been shown to exhibit anticancer properties and are known to be potent

*To whom correspondence should be addressed. E-mail: turro@chemistry.ohio-state.edu.

(1) Kessel, D.; Dougherty, T. J. *Rev. Contemp. Pharmacother.* **1999**, *10*, 19–24.
(2) DeRosa, M. C.; Crutchley, R. J. *Coord. Chem. Rev.* **2002**, *233*−*234*, 355–371.
(3) Dalla, V.; Lisa, M.; Sebastiano, M. *Curr. Med. Chem.* **2001**, *8*, 1405–1418.
(4) Allen, C. M.; Sharman, W. M.; van Lier, J. E. *Tumor Targeting Cancer Ther.* **2002**, 329–361.
(5) Hsi, R. A.; Rosenthal, D. I.; Glatstein, E. *Drugs* **1999**, *57*, 725–734.
(6) McCaughan, J. S., Jr. *Drugs Aging* **1999**, *15*, 49–68.
(7) Detty, M. R.; Gibson, S. L.; Wagner, S. *J. Med. Chem.* **2004**, *47*, 3897–3915.
(8) (a) Harris, A. L. *Nat. Rev. Cancer* **2002**, *2*, 38–47. (b) Shannon, A. M.; Bouchier-Hayes, D. J.; Condron, C. M.; Toomey, D. *Cancer Treat. Rev.* **2003**, *29*, 297–307. (c) Guppy, M. *Biochem. Biophys. Res. Commun.* **2002**, *299*, 676–680. (d) Knowles, H. J.; Harris, A. L. *Breast Cancer Res.* **2001**, *3*, 318–322.
(9) (a) Sorasaenee, K.; Fu, P. K.-L.; Angeles-Boza, A. M.; Dunbar, K. R.; Turro, C. *Inorg. Chem.* **2003**, *42*, 1267–1271. (b) Chifotides, H. T.; Fu, P. K.-L.; Dunbar, K. R.; Turro, C. *Inorg. Chem.* **2004**, *43*, 1175–1183. (c) Aguirre, J. D.; Lutterman, D. A.; Angeles-Boza, A. M.; Dunbar, K. R.; Turro, C. *Inorg. Chem.* **2007**, *46*, 7494–7502. (d) Aguirre, J. D.; Chifotides, H. T.; Angeles-Boza, A. M.; Chouai, A.; Turro, C.; Dunbar, K. R. *Inorg. Chem.* **2009**, *48*, 4435–4444.

Published on Web 05/24/2010

inhibitors of transcription.[9] Complexes possessing ligands with extended π-systems exhibit activity toward HeLa and COLO-316 cancer cell lines, making these types of compounds useful as potential antitumor agents.[10,11] Specifically, dirhodium(II,II) complexes based on the dipyrido[3,2-*a*:2′, 3′-*c*]phenazine (dppz) ligand were previously shown to exhibit an increase in toxicity upon irradiation similar to that of hematoporphyrin, a component in the PDT drug Photofrin.[12,13] In addition, the DNA photocleavage by *cis*-$[Rh_2(\mu\text{-}O_2CCH_3)_2(dppz)_2]^{2+}$ and *cis*-$[Rh_2(\mu\text{-}O_2CCH_3)_2$-$(bpy)(dppz)]^{2+}$ (bpy = 2,2′-bipyridine) was still active in the absence of oxygen,[12−14] making these complexes potential candidates for oxygen-independent PDT. Furthermore, studies relating the intercalation of ligands with extended π-systems to DNA photocleavage show evidence of enhanced reactivity in complexes that bind strongly to the double helix.[15] Therefore, it is desirable to synthesize related complexes that maintain the ability to photocleave in the absence of oxygen and are intercalators.[12]

The present work focuses on a related series of complexes, *cis*-$[Rh_2(\mu\text{-}O_2CCH_3)_2(dppn)(L)]^{2+}$, where dppn = benzo[*i*]-dipyrido[3,2-*a*:2′,3′-*c*]phenazine and L = bpy (**1**), phen (1,10-phenanthroline, **2**), dpq (dipyrido[3,2-*f*:2′,3′-*h*]quinoxaline, **3**), dppz (dipyrido [3,2-*a*:2′,3′-*c*] phenazine, **4**), and dppn (**5**). A schematic representation of the molecular structures of the complexes and ligands is depicted in Figure 1. The photophysical properties of the complexes and their ability to bind and photocleave DNA were probed, along with their toxicity toward human skin cells in the dark and when irradiated with visible light. The known ability of **1**−**5** to transverse cellular membranes, their toxicity in the dark, and their photophysical properties were used to explain the observed results.

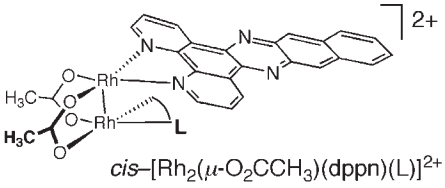

cis–$[Rh_2(\mu\text{-}O_2CCH_3)(dppn)(L)]^{2+}$

Complex	L
1	bpy
2	phen
3	dpq
4	dppz
5	dppn

Figure 1. Molecular structure of the dirhodium complexes showing numbering scheme and ligand structures.

Experimental Section

Materials. Sodium chloride, sodium phosphate, gel loading buffer (0.05% (w/v) bromophenol blue, 40% (w/v) sucrose, 0.1 M EDTA (pH = 8.0, 0.5% (w/v) sodium lauryl sulfate), Trizma base, Tris/HCl, and ethidium bromide were purchased from Sigma and used as received. Calf thymus DNA was purchased from Sigma and was dialyzed against a 5 mM Tris, 50 mM NaCl (pH = 7.5) buffer three times during a 48 h period prior to use. The pUC18 plasmid was purchased from Bayou Biolabs and purified using the QIAprep Spin Miniprep Spin System from Qiagen. Methanol and dichloromethane were dried over CaH_2 and distilled under a nitrogen atmosphere prior to use. 1,3-Diphenylisobenzofuran (DPBF) and polystyrene sulfonate (PSS) were purchased from Aldrich and used without further purification. Compounds **1**−**5** were synthesized by previously reported methods.[10]

Instrumentation. Steady-state absorption spectra were recorded on a Perkin-Elmer Lambda 900 spectrometer or a HP diode array spectrometer (HP8453) with HP8453 Win System software. Corrected steady-state emission spectra were measured on a SPEX Fluoromax-2 luminescence spectrometer. The home-built transient absorption instrument for measurements on the nanosecond and microsecond time scales was previously reported, using a frequency-tripled (355 nm) Spectra-Physics GCR-150 Nd:YAG laser (fwhm ~8 ns) as the excitation source.[16] A 150 W Xe arc lamp in a PTI housing (Milliarc compact lamp housing) powered by an LPS-220 power supply (PTI) with an LPS- 221 igniter (PTI) was used for the DNA photocleavage experiments. The irradiation wavelength was selected by placing long-pass colored glass filters (Melles Griot) and a 10 cm water cell in the light path. The ethidium bromide-stained agarose gels were imaged using a Gel Doc 2000 transilluminator (BioRad) equipped with Quantity One (v. 4.1.1) software

Methods. The DNA photocleavage experiments were carried out with a 10 or 20 μL total sample volume in 0.5 mL transparent Eppendorf tubes containing 100 μM pUC18 plasmid and 20 μM of each metal complex. Irradiation of the solutions was performed either in air or after six freeze−pump−thaw cycles in quartz tubes equipped with a Kontes stopcock (using ~3-fold greater solution volume). Following irradiation, 4 μL of the DNA gel loading buffer was added to each sample. The electrophoresis was carried out using a 1% agarose gel stained with 0.5 mg/L ethidium bromide in 1× TAE buffer (40 mM tris-acetate, 1 mM EDTA, pH ~8.2); other conditions are specified as needed. Using Quantity One software, background-corrected intensity values of both form I (undamaged, supercoiled) and form II (single-strand break, nicked, circular) bands for each lane were calculated. The sum of the total intensity found for both forms I and II was taken as the total sample intensity, and percent photocleavage of each sample was calculated to be the percent intensity of form II. The binding constants of the metal complexes to calf thymus DNA determined by optical titrations at room temperature were measured with 5 μM metal complex,

(10) Aguirre, J. D.; Angeles-Boza, A. M.; Chouai, A.; Turro, C.; Pellois, P.; Dunbar, K. R. *Dalton Trans.* **2009**, *48*, 10806–10812.
(11) Aguirre, J. D.; Angeles-Boza, A. M.; Chouai, A.; Pellois, J.-P.; Turro, C.; Dunbar, K. R. *J. Am. Chem. Soc.* **2009**, *131*, 11353–11360.
(12) Angeles-Boza, A. M.; Bradley, P. M.; Fu, P. K.-L.; Wicke, S. E.; Bacsa, J.; Dunbar, K. R.; Turro, C. *Inorg. Chem.* **2004**, *43*, 8510–8519.
(13) Angeles-Boza, A. M.; Bradley, P. M.; Fu, P. K.-L.; Shatruk, M.; Hilfiger, M. G.; Dunbar, K. R.; Turro, C. *Inorg. Chem.* **2005**, *44*, 7262–7264.
(14) Bradley, P. M.; Angeles-Boza, A. M.; Dunbar, K. R.; Turro, C. *Inorg. Chem.* **2004**, *43*, 2450–2452.
(15) Gao, F.; Chao, H.; Ji, L.-N. *Chem. Biodiversity* **2008**, *5*, 1962–1979.
(16) Warren, J. T.; Chen, W.; Johnston, D. H.; Turro, C. *Inorg. Chem.* **1999**, *38*, 6187–6192.

and the calf thymus DNA concentration was varied from 0 to 100 μM (5 mM Tris/HCl, 50 mM NaCl, pH = 7.5). The dilution of metal complex concentration at the end of each titration was negligible. The DNA binding constant, K_b, was obtained from fits of the titration data, as previously reported.[12,17]

Photophysical measurements were performed in a 1 × 1 cm quartz cuvette equipped with a rubber septum, and the solutions were bubbled with argon for 15 min prior to each measurement, unless otherwise noted. For determination of $\Phi_{^1O_2}$, deareated solutions with concentrations adjusted to obtain absorption of 0.05 at the irradiation wavelength (λ_{exc} = 450 nm) were used. The quantum yield of singlet oxygen produced by each complex was measured relative to $[Ru(bpy)_3]^{2+}$ as the standard ($\Phi_{^1O_2}$ (0.81 in CH_3OH),[18] by monitoring the fluorescence quenching of DPBF (λ_{exc} = 405 nm), a known $^1O_2$ target.[19] Under these conditions, the plot of fluorescence intensity of DPBF versus irradiation time yields a slope that can be compared relative to that of the standard and used to calculate $\Phi_{^1O_2}$ for each complex.

Human skin fibroblasts (Hs-27) were obtained from the American Type Culture Collection, cell line CRL-1634 (Manassas). Cells were cultured in Dulbecco's modified Eagle medium, containing 10% fetal bovine serum (Invitrogen Life Technologies), 50 μg/mL gentamicin, 4.5 mg/mL glucose, and 4 mM L-glutamine (Invitrogen Life Technology). Cell cultures were incubated in a humidified atmosphere containing 5% CO_2 at 37 °C. For assessing the cytotoxicity and photocytotoxicity of different compounds, subconfluent (50−80% confluent) monolayers of Hs-27 in 60 mm culture dishes were used. The monolayers were washed twice with phosphate-buffered saline (PBS) to ensure that the culture dishes were free of any culture medium, after which time fresh PBS containing different concentrations of each compound was added to cover the fibroblasts. The cells were irradiated through the PBS buffer, which does not absorb light in the visible region. After irradiation, the cells were removed from the dishes by trypsinization, seeded into 24-well culture plates, and incubated for 2 to 4 days or until the untreated control group reached confluence. *N*-Lauroyl sarcosine (200 μL, 40 mM) was then added to each well, and the cells were allowed to lyse for at least 15 min. Quantitative determination of the protein content in each well was undertaken using Peterson's modification of the micro-Lowry method (Sigma reagent kit),[20] where the lysate was treated with 200 μL of Lowry reagent for 20 min and then with 100 μL of Folin-Ciocalteu phenol reagent for 30 min or until color developed. A portion of the contents (200 μL) of each well was transferred to a 96-well plate for absorbance determination using a multiwell plate reader (Dynatech Laboratory). The absorbance at 630 nm was monitored, which is proportional to the total protein content and the number of cells in each well.

Results and Discussion

Photophysical Properties. The electronic absorption maxima of **1**−**5** are listed in Table 1. Complexes **1**−**5** exhibit ligand-centered (LC) transitions with maxima in the 250 to 430 nm range in water. By comparison, the free dppn ligand exhibits absorption maxima at 318 nm (65 000 M^{-1} cm^{-1}), 390 nm (9400 M^{-1} cm^{-1}), and 414 nm (12 500 M^{-1} cm^{-1}) in $CHCl_3$.[21] Similarly, the related tridentate ligand, 3-(pyrid-2′-yl)-4,5,9,16-tetraazadibenzo[*a*,*c*]naphthacene (pydppn), exhibits comparable LC transitions at 329 nm (66 000 M^{-1} cm^{-1}), 398 nm (13 000 M^{-1} cm^{-1}), and 421 nm (17 000 M^{-1} cm^{-1}) in $CHCl_3$.[22] Absorption maxima in the ranges 259−272 and 316−329 nm are observed in **1**−**5**, which can be associated with ligand-centered transitions of the free ligands in each complex. For example, from comparison to the spectral features of the free dppn ligand, the absorption features observed at 316−329 nm in **1**−**5** are assigned to transitions of dppn. A metal-to-ligand charge transfer (MLCT) transition is observed in the related complexes *cis*-$[Rh_2(\mu\text{-}O_2CCH_3)_2(bpy)_2]^{2+}$, *cis*-$[Rh_2(\mu\text{-}O_2CCH_3)_2(bpy)(dppz)]^{2+}$, and *cis*-$[Rh_2(\mu\text{-}O_2CCH_3)_2(dppz)_2]^{2+}$ with maxima at 408 nm (ε = 2920 M^{-1} cm^{-1}),[23] 432 nm (3100 M^{-1} cm^{-1}), and 434 nm (5460 M^{-1} cm^{-1}),[12,13] respectively, which is also expected to be present in **1**−**5**. It is likely that this MLCT peak is indeed present, but is obscured by the dppn features in this region because it is weaker than the LC transitions in this spectral range. In addition, complexes **1**−**5** exhibit a significantly weaker metal-centered (MC) RhRhπ*→RhRhσ* transition with maxima at ∼600−621 nm. This MC transition is also observed in *cis*-$[Rh_2(\mu\text{-}O_2CCH_3)_2(bpy)_2]^{2+}$ and $Rh_2(\mu\text{-}O_2CCH_3)_4$ at 512 nm (ε = 380 M^{-1} cm^{-1})[23] and 585 nm (ε = 241 M^{-1} cm^{-1}), respectively.[24] As was previously reported for the related complexes *cis*-$[Rh_2(\mu\text{-}O_2CCH_3)_2(bpy)(dppz)]^{2+}$ and *cis*-$[Rh_2(\mu\text{-}O_2CCH_3)_2(dppz)_2]^{2+}$,[12] complexes **1**−**5** are nonemissive at 298 K in water.

Table 1. Absorption Maxima, Sensitized Singlet Oxygen Quantum Yields, and Transient Absorption Lifetimes of **1**−**5**

complex	λ_{abs}/nm ($\varepsilon \times 10^{-3}$/$M^{-1}$ cm^{-1})[a]	$\Phi_{^1O_2}$[b]	τ/μs[c]
1	259 (38.5), 270 (37.9), 323 (45.4), 405 (9.4), 600 (1.6)	0.7	2.7
2	261 (60.5), 325 (59.7), 406 (10.7), 618 (1.6)	0.9	2.4
3	259 (57.1), 318 (39.6), 409 (7.9), 609 (1.1)	0.8	2.4
4	272 (36.7), 329 (25.3), 390 (13.6), 430 (9.9), ∼620 (3.8)	0.4	3.5
5	260 (60.5), 316 (67.0), 410 (13.2), 621 (2.0)	0.4	4.1

[a] In water. [b] In methanol (λ_{irr} = 450 nm). [c] In deareated DMSO (λ_{exc} = 355 nm, fwhm ∼8 ns).

Although **1**−**5** are not emissive, the complexes exhibit a long-lived excited state observed by transient absorption spectroscopy. The transient absorption spectra of **2** and **3** are shown in Figure 2 in deaerated DMSO (λ_{exc} = 355 nm), with spectral features similar to those of **1**, **4**, and **5**. The transient absorption spectra of **1**−**5** in DMSO exhibit a peak at ∼430 nm, broad bands with maxima at 520−540 nm, with monoexponential decay lifetimes of 2.4 to 4.1 μs (Table 1). A similar transient absorption signal was observed for 25 μM free dppn ligand in deoxygenated $CHCl_3$ (λ_{exc} = 355 nm), with a broad maximum at 540 nm

(17) Liu, Y.; Hammitt, R.; Lutterman, D. A.; Thummel, R. P.; Turro, C. *Inorg. Chem.* **2007**, *46*, 6011–6021.
(18) Bhattacharyya, K.; Das, P. K. *Chem. Phys. Lett.* **1985**, *116*, 326–332.
(19) (a) Roitman, L.; Ehrenberg, B.; Kobayashi, N. *J. Photochem. Photobiol. A: Chem.* **1994**, *77*, 23–28. (b) Spiller, W.; Kliesch, H.; Wohrle, D.; Hackbarth, S.; Roder, B.; Schnurpfeil, G. *J. Porphyrins Phthalocyanines* **1998**, *2*, 145–158. (c) Ding, H.-Y.; Wang, X.-S.; Song, L.-Q.; Chen, J.-R.; Yu, J.-H.; Li, C.; Zhang, B.-W. *J. Photochem. Photobiol. A: Chem.* **2006**, *177*, 286–294.
(20) (a) Peterson, G. L. *Analyt. Biochem.* **1977**, *83*, 346–356. (b) Bensadoun, A.; Weinstein, D. *Anal. Biochem.* **1976**, *70*, 241–250. (c) Lowry, O. H.; Roseberough, N. J.; Farr, A. L.; Randall, R. J. *J. Biol. Chem.* **1951**, *193*, 265–275.
(21) Sun, Y.; Collins, S.; Joyce, L. E.; Turro, C. *Inorg. Chem.* **2010**, *46*, 2426–2428.
(22) Liu, Y.; Hammitt, R.; Lutterman, D. A.; Joyce, L. E.; Thummel, R. P.; Turro, C. *Inorg. Chem.* **2009**, *48*, 375–385.
(23) Crawford, C. A.; Matonic, J. H.; Huffman, J. C.; Folting, K.; Dunbar, K. R.; Christou, G. *Inorg. Chem.* **1997**, *36*, 2361–2371.
(24) Sowa, T.; Kawamura, T.; Shida, T.; Yonezawa, T. *Inorg. Chem.* **1983**, *22*, 56–61.

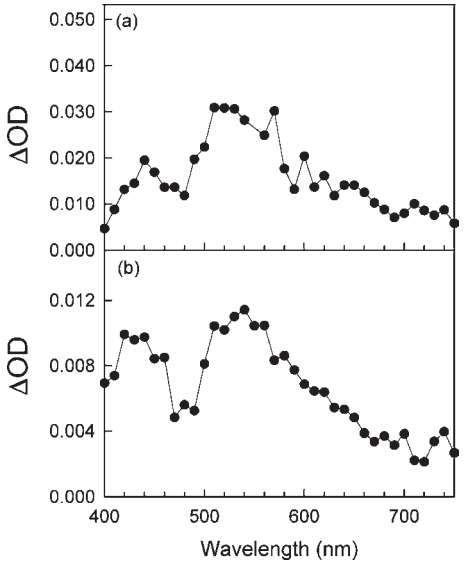

Figure 2. Transient absorption spectra of (a) 0.15 mM **2** and (b) 0.30 mM **3** in DMSO collected 20 ns after the excitation pulse (λ_{exc} = 355 nm, fwhm ~8 ns).

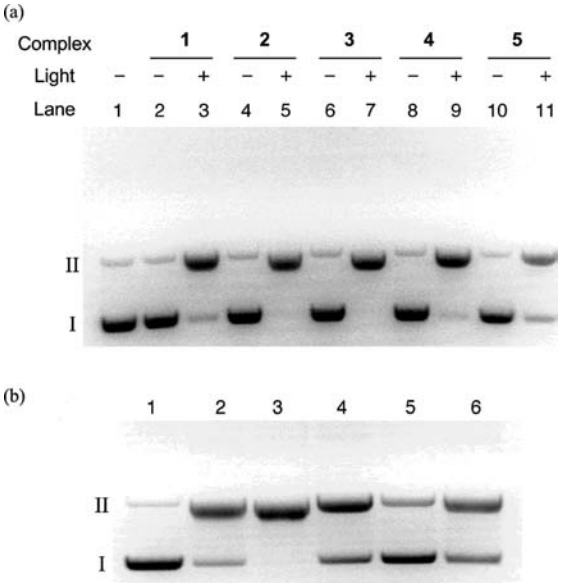

Figure 3. Ethidium bromide-stained agarose gels with 100 μM pUC18 plasmid and 20 μM complex (5 mM Tris, pH = 7.5, 50 mM NaCl). (a) Photocleavage by **1**−**5** in air ($\lambda_{irr} \geq 375$ nm, 20 min), where lanes 1, 2, 4, 6, 8, and 10 are dark controls and lanes 3, 5, 7, 9, and 11 are irradiated: lane 1, plasmid only; lanes 2 and 3, **1** ; lanes 4 and 5, **2**; lanes 6 and 7, **3**; lanes 8 and 9, **4**; lanes 10 and 11, **5**. (b) Photocleavage by **4** ($\lambda_{irr} > 385$ nm, 12 min): lane 1, plasmid only, dark; lane 2, irr. in air; lane 3, irr. in D_2O; lane 4, irr. with 2 mM NaN_3; lane 5, irr. after six freeze−pump−thaw cycles; lane 6, irr. with 2 units SOD.

and τ = 13.0 μs. An increase in the transient absorption signal at $\lambda < 420$ nm is also observed for free dppn. The apparent shift in the maximum of this peak to lower energies in **1**−**5** is explained by the overlap of the ground state absorption bleach with maxima at ~410 nm contributing to the transient absorption signal. On the basis of the comparison of the maxima and lifetimes of the transient absorption signals of **1**−**5** to those measured for the free dppn ligand, the excited state observed for the dirhodium complexes is assigned as arising from the $^3\pi\pi^*$ centered on the dppn ligand.

Since the mechanism of action of PDT agents currently in use relies on the production of $^1O_2$, the quantum yield of photosensitized $^1O_2$ production ($\Phi_{^1O_2}$) for **1**−**5** was measured in methanol (Table 1). For the sake of comparison, it is noted that Photofrin has $\Phi_{^1O_2} = 0.17$.[25] It is interesting to note that $\Phi_{^1O_2}$ for **1**−**3** is ~2-fold greater than those for **4** and **5**. This trend is unexpected, since the excited state lifetimes of **4** and **5** are longer than those of **1**−**3**, which should result in greater photosensitization of $^1O_2$ in the former. A possible explanation for the difference in $\Phi_{^1O_2}$ is the aggregation of the more hydrophobic **4** and **5** in alcohols and water, a trend that has been reported for cationic complexes of Ru(II) and Rh_2(II,II) possessing ligands with extended π-systems.[12,13]

DNA Binding and Photocleavage. Prior relative viscosity experiments revealed that, with lower concentrations of complex (up to 60 μM) and DNA (200 μM DNA), **1** and **2** intercalate between the DNA bases effectively, but **3**−**5** do not.[10] By using greater concentrations of the probe (up to 300 μM) and 1 mM DNA, some intercalation by **3** and **4** is also apparent (Supporting Information). Relative viscosity measurements of **5** at high concentration were not possible owing to the lower solubility of this complex. Owing to the juxtaposed nature of the two dppn ligands on the complex and the results from the relative viscosity measurements at low concentrations, it is believed that **5** does not intercalate between the DNA bases. A lack of change in viscosity upon increased concentrations of complex was previously reported for the related complexes *cis*-$[Rh_2(\mu\text{-}O_2CCH_3)_2(bpy)(dppz)]^{2+}$ and *cis*-$[Rh_2(\mu\text{-}O_2CCH_3)_2(dppz)_2]^{2+}$, which are not intercalators.[12,13]

Changes in the absorption spectra of **1**−**5** upon addition of DNA were also observed. These hypochromic and bathochromic shifts are often associated with intercalation of the complexes, however, aggregation of cationic hydrophobic complexes enhanced by the presence of the polyanionic DNA backbone has a similar effect.[12,26,27] In order to distinguish between these two mechanisms, the changes in absorption of **1**−**5** were also recorded in the presence of a similar concentration of the random-coil polyanion polystyrene sulfonate (PSS). A comparison of the absorption spectra recorded in the presence of 100 μM DNA (bases) and 100 μM PSS reveals that **1**−**3** indeed intercalate between the DNA bases, whereas the absorption shifts observed for **4** and **5** are a result of enhanced aggregation effected by the polyanion. Complex **3** exhibits absorption changes due to contributions from both intercalation and aggregation. The shifts in the absorption of **1** and **2** as a function of DNA concentration were used to estimate their DNA binding constants, resulting in values of 1.2×10^6 and 1.0×10^5 M^{-1}, respectively. The values are consistent with those of other intercalators.[26,27]

Figure 3a compares the photocleavage of 100 μM pUC18 plasmid DNA in air in the presence of **1**−**5**. The plasmid-only control is shown in lane 1, illustrating the mobility of both the major supercoiled form (form I) and the trace nicked, circular form (form II) present in the

(25) Gottfried, V.; Peled, D.; Winkelman, J. W.; Kimel, S. *Photochem. Photobiol.* **1988**, *48*, 157–163.

(26) Nair, R. B.; Teng, E. S.; Kirkland, S. L.; Murphy, C. J. *Inorg. Chem.* **1998**, *37*, 139–141.

(27) Tang, T.-C.; Huang, H.-J. *Electroanalysis* **1999**, *11*, 1185–1190.

Table 2. DNA Photocleavage, LC_{50} Values Irradiated and in the Dark, and Partition Coefficients for **1**−**5**

		$LC_{50}/\mu M$[a]			
complex	% form II[a]	dark	irradiated[b]	increase	log(*P*)[c]
1	64	200 ± 20	30 ± 5	6.7	0.32
2	68	178 ± 17	22 ± 4	8.1	0.30
3	66	51 ± 5	9 ± 3	5.7	0.41
4	66	355 ± 18	17 ± 3	21	0.62
5	43	384 ± 24	16 ± 4	24	1.02

[a] See text; 5% error. [b] λ_{irr} = 400−700 nm, 30 min. [c] From ref 10, ±0.03.

samples. It is clear from Figure 3a that none of the complexes cleave DNA in the dark, but **1**−**4** efficiently generate single-strand breaks (SSBs, form II) upon irradiation with visible light ($\lambda_{irr} \geq 375$ nm) for 20 min with percent formation of form II ranging from 64% to 68% (Table 2). Irradiation of **5** in air results in significantly lower DNA photocleavage, 43%, compared to **1**−**4** under similar irradiation conditions (Figure 3a, lane 11). For complexes **1**−**4**, the DNA photocleavage is associated with the formation of reactive oxygen species, as illustrated by the DNA photocleavage of **4** under various experimental conditions shown in Figure 3b. Lane 3 shows greater photocleavage in D_2O compared to H_2O (lane 2), indicative that $^1O_2$ plays a role in the reactivity, since the lifetime of $^1O_2$ is 3-fold greater in D_2O than H_2O.[28] The addition of known radical and reactive oxygen species scavengers, sodium azide (lane 3) and superoxide dismutase (SOD, lane 5), as well as subjecting the sample to six freeze−pump−thaw (FPT) cycles (lane 4), thereby rendering the sample devoid of oxygen, result in decreased cleavage.[28] As was previously reported for related dirhodium complexes, there appears to be a dominant O_2-dependent pathway and minor O_2-independent reactivity.[12] The results shown in Figure 3b for **4** are representative of those also measured for **1**−**3**. The DNA photocleaveage by **5** is relatively invariant in D_2O, after FPT cycles, and in the presence of azide and SOD, results that support a DNA damage mechanism that is independent of oxygen. Since the quantum yields of photosensitized $^1O_2$ are similar for **4** and **5**, the difference in DNA photocleavage ability of the two complexes can be attributed to the ability of **4** to partially intercalate between the DNA bases, thus generating $^1O_2$ within the DNA local environment. Given the fact that **5** does not intercalated between the DNA bases, $^1O_2$ produced upon irradiation is likely not in the vicinity of the duplex.

Toxicity and Phototoxicity. The toxicity of **1**−**5** toward two cancer cell lines, HeLa and COLO-316, was previously investigated in the dark.[10] The data revealed that **1**−**4** induce apoptosis, whereas **5** does not. It is believed that, owing to its hydrophobicity, **5** does not transverse the cellular membrane as well as the other complexes. Furthermore, the toxicity of complexes **1** and **5** in the dark toward Hs-27 human skin fibroblasts was previously examined in relation to the partition coefficient of each complex,[29] also known to be related to the ability of molecules to transverse cellular membranes.[10] A similar result is observed with the Hs-27 cell line presented here, where complexes **4** and **5** exhibit significantly lower toxicity in the dark, with LC_{50} (LC_{50} = concentration required to kill 50% of the cells) values of 355 and 384 μM, respectively, compared to 51−200 μM for **1**−**3** (Table 2). For the Hs-27 cell line, it appears that complexes **4** and **5** do not transverse the cellular membrane as well as **1**−**3**. This trend is supported by the partition coefficients (*P*) previously reported, also listed in Table 2 as log(*P*), which show that **4** and **5** are significantly more hydrophobic than **1**−**3**. Although the log *P* value for **4** is closer to **1**−**3** than **5**, it has been previously noted that a linear progression of permeability with ring additions is not followed in this series of complexes possibly due to the direct stacking of the diimine ligands.[10]

In addition to the ability to enter cells, photocytotoxicity also depends on the reactivity of each complex when excited with light. The LC_{50} values for **1**−**5** irradiated for 30 min with visible light show that the most and least phototoxic compounds are **3** and **1**, respectively, and **2**, **4**, and **5** exhibit similar toxicities. It is possible that the more hydrophobic complexes **4** and **5** are bound within the cellular membrane, and photoexcitation initiates reactivity toward phospholipids, ultimately resulting in cell death.[30] In contrast, complexes **1**−**3** are able to penetrate the cellular membrane and can, therefore, damage intracellular components through the formation of reactive oxygen species. Work is currently underway to elucidate the differences in mechanism for these systems.

The values of the increase in toxicity toward Hs-27 of **1**−**5** upon irradiation are listed in Table 2, ranging from 5.7- to 8.1-fold for **1**−**3**. These values are similar to the 5.5-fold increase previously measured by us for hematoporphyrin, a key component of the PDT drug Photofrin, under similar experimental conditions, with LC_{50}^{dark} = 22 ± 1 μM and LC_{50}^{irr} = 3.8 ± 0.2 μM. In contrast, the increase in toxicity of **4** and **5** when irradiated was measured to be 21 and 24, respectively, making them potential candidates for PDT. It should be noted that this greater increase in **4** and **5** compared to hematoporphyrin reflects the lower toxicity of the complexes in the dark, a desirable property for a PDT agent.

Conclusions

The photophysical properties of the series of complexes *cis*-$[Rh_2(\mu\text{-}O_2CCH_3)_2(dppn)(L)]^{2+}$ (L = bpy (**1**), phen (**2**), dpq (**3**), dppz (**4**), and dppn (**5**)) were investigated, and it was found that the lowest energy excited state in **1**−**5** is dppn-localized $^3\pi\pi^*$ with lifetimes of 2.4−4.1 μs in DMSO. Complexes **1**−**4** photocleave DNA efficiently via a mechanism mediated by reactive oxygen species, whereas the lower reactivity of **5** toward DNA is independent of the presence of oxygen. It should be noted, however, that all complexes also exhibit a photocleavage pathway that is independent of oxygen. Therefore, a direct comparison of the DNA photocleavage efficiency and quantum yield of photosensitized $^1O_2$ production is not possible. The toxicity of **1**−**5** toward Hs-27 human skin fibroblasts is significantly enhanced upon irradiation with visible light as compared to in the dark, with a 21- and 24-fold increase in toxicity for **4** and **5**, respectively. This increase is significantly greater than that measured

(28) Rosenthal, I.; Ben-Hur, E. *Int. J. Radiat. Biol.* **1995**, *67*, 85–91.
(29) Angeles-Boza, A. M.; Chifotides, H. T.; Aguirre, J. D.; Chouai, A.; Fu, P. K.-L.; Dunbar, K. R.; Turro, C. *J. Med. Chem.* **2006**, *49*, 6841–6847.
(30) Girotti, A. W. *Compr. Ser. Photosci.* **2001**, *3*, 233–250.

under similar experimental conditions for hematoporphyrin (5.5-fold). The dramatic increase in toxicity upon irradiation of **4** and **5** makes them potentially useful as PDT agents. Experiments designed to gain further understanding of the mechanism of photoinduced cell death in the presence of these complexes are currently underway.

Acknowledgment. C.T. and K.R.D. thank the National Science Foundation (CHE-0911354) for partial support of this work.

Supporting Information Available: Relative viscosity changes. These materials are available free of charge via the Internet at http://pubs.acs.org.